Energy-Efficient IRS-Aided NOMA Beamforming for 6G Wireless Communications

Asim Ihsan[ID], Wen Chen[ID], *Senior Member, IEEE*, Muhammad Asif[ID], Wali Ullah Khan[ID], *Member, IEEE*, Qingqing Wu[ID], *Senior Member, IEEE*, and Jun Li[ID], *Senior Member, IEEE*

Abstract—This manuscript presents an energy-efficient alternating optimization framework based on intelligent reflective surfaces (IRS) aided non-orthogonal multiple access beamforming (NOMA-BF) system for 6G wireless communications. Specifically, this work proposes a centralized IRS-enabled design for the NOMA-BF system to optimize the active beamforming and power allocation coefficient (PAC) of users at the transmitter in the first stage and passive beamforming at IRS in the 2nd stage to maximize the energy efficiency (EE) of the network. However, an increment in the number of supportable users with the NOMA-BF system will lead to NOMA user interference and inter-cluster interference (ICI). To mitigate the effect of ICI, first zero-forcing beamforming along with efficient user clustering algorithm is exploited and then NOMA user interference is tackled efficiently through a proposed iterative algorithm that computes PAC of NOMA user through simplified closed-form expression under the required system constraints. In the 2nd stage, the problem of passive beamforming is solved through a technique based on difference-of-convex (DC) programming and successive convex approximation (SCA). Simulation results demonstrate that the proposed alternating framework for energy-efficient IRS-assisted NOMA-BF system can achieve convergence within a few iterations and provide efficient performance in terms of EE of the system with low complexity.

Asim Ihsan and Wen Chen are with the Department of Information and Communication Engineering, Shanghai Jiao Tong University, Shanghai 200240, China (e-mail: ihsanasim@sjtu.edu.cn; wenchen@sjtu.edu.cn).

Muhammad Asif is with the Guangdong Key Laboratory of Intelligent Information Processing, College of Electronics and Information Engineering, Shenzhen University, Shenzhen 518000, Guangdong, China (e-mail: masif@szu.edu.cn).

Wali Ullah Khan is with the Interdisciplinary Centre for Security, Reliability and Trust, University of Luxembourg, 1855 Luxembourg City, Luxembourg (e-mail: waliullah.khan@uni.lu).

Qingqing Wu is with the State Key Laboratory of Internet of Things for Smart City, University of Macau, Macau, China, and also with the Guangdong-Macau Joint Laboratory for Advanced and Intelligent Computing, Guangzhou, China (e-mail: qingqingwu@um.edu.mo).

Jun Li is with the School of Electronic and Optical Engineering, Nanjing University of Science and Technology, Nanjing 210094, China (e-mail: jun.li@njust.edu.cn).

Digital Object Identifier 10.1109/TGCN.2022.3209617

I. Introduction and Motivations

THE WIRELESS generations from 1G to 5G are designed through the assumption that the wireless environment cannot be controlled and modified. Therefore it can only be compensated through the design of efficient transmission/reception technologies. However, the enhancements at the endpoints of the wireless communications are not enough to meet the quality of services requirements of beyond 5G networks. Instead, 6G vision can be achieved by treating the wireless environment as an adaptable variable that is to be optimized. This can be possible through the use of Intelligent Reflective Surfaces (IRSs), which are known as enabling technology for 6G [1]. The 6G plan to serve billions of interconnected devices for applications like smart homes, cities and transportation through IRS would require advanced energy and spectral efficient resource allocation frameworks.

IRSs have attracted considerable attention for their efficient control over electromagnetic waves. IRS contains an integrated electronic circuit with software that can control the propagation characteristics of the electromagnetic channel in a customizable way. It is a cost-effective technology for enhancing the energy and spectral efficiency of beyond 5G wireless communication which can be used in various new use cases. These include the utilization of IRS as a passive reflector, in which IRS operates without the connection of radio frequency (RF) chains and require very little power to control the tunable chips. The passive IRS can be deployed with scalable cost, lower energy consumption, and without sophisticated interference management [2]. Besides it, Active IRS is connected with radio frequency (RF) chains and can be used as active holographic MIMO which is the next step beyond massive MIMO because it has the potential to exploit the propagation characteristics of the electromagnetic channel with very low complexity in practical [3], [4]. Moreover, IRS has many favourable properties like the ease in integration into currently existing wireless networks and can be deployed on the buildings, roadside billboards, windows and indoor walls. These properties attracted researchers to investigate the benefits of IRS aided wireless communications, such as the transmit power minimization [5], interference reduction [6] and security enhancement [7].

Non-orthogonal multiple access (NOMA) is a prominent multiple access candidate of the next-generation multiple access (NGMA) family for the 6G network [8], [9]. The 6G network is expected to serve terrestrial, aerial, and maritime communications in a more swift, efficient and reliable manner. Moreover, it can support billions of interconnected devices with ultra-low latency requirements for applications like smart homes, cities and transportation. To meet these expected targets of 6G, NOMA is of great importance. NOMA has attracted much attention from both academia and industry because of its high spectral efficiency, grants free access to the networks, and user fairness. It mitigates resource collisions due to its high overloading transmissions through limited resources [9], thereby enhancing spectral efficiency and reducing latency [8]. The integration of NOMA with IRS can achieve enhanced massive connectivity with higher spectral and energy efficiency. Moreover, IRS enabled NOMA networks are more adaptable than conventional NOMA networks because IRS can smartly adjust the direction of a channel vector of receivers, which assists in the implementation of NOMA [10]. In addition, IRS consist of multiple reflecting elements which can relax the strict constraint on the number of antennas at the transmitter and receiver in multiple antennas network [8]. The above-mentioned merits of IRS-NOMA have drawn considerable research interest and several studies have been conducted. For instance, the authors in [11] minimized the transmit power of the IRS-NOMA system by optimizing the beamforming vectors at BS and phase shift matrix at the IRS. In [10], the performance of IRS assisted NOMA transmissions are described and investigated the influence of hardware impairments on their proposed design of IRS-NOMA system. Under the assumption of ideal and non-ideal IRS, the sum rate of the system is maximized in [12] by the joint optimization of active beamforming at the source and passive beamforming at the IRS. The transmit power of IRS assisted multi-cluster MISO NOMA network is minimized in [13]. The detailed comparison between IRS-NOMA with IRS-OMA is presented in [14]. Moreover, the interplay between IRS and NOMA is widely investigated for various technologies like unmanned aerial vehicle (UAV) [15], simultaneous wireless information and power transfer (SWIPT) [16], wireless powered communication networks (WPCNs) [17], mobile edge computing (MEC) [18], Backscatter Communications (BC) [19], and physical layer security (PLS) [20].

To enable the Internet of Everything (IoE) applications through 6G wireless systems will result in a massive number of connections and huge data traffic. Therefore, the realization of IoE will require to gain high spectral efficiency [21]. To further improve the sum capacity for future IoE applications, NOMA-BF can be exploited that can support multiple users in each cluster using a single BF vector through NOMA principles [22]. As IRS can smartly adjust the direction of a channel vector of receivers and it can also relax the strict constraint on the number of antennas at the transmitter and receiver in multiple antennas network. Therefore, it can be a prominent choice for the realization of IoE applications through NOMA-BF systems. The implementation of IRS aided NOMA-BF systems can be possible through centralized IRS-enabled design [23], [24].

Inspired and motivated by the above research contributions, the energy-efficient IRS-aided NOMA-BF system for 6G wireless communications is proposed in this paper. Our major contribution is summarized as follows,

1) *Energy-efficient centralized IRS NOMA-BF design:* The realization of IoE applications through 6G wireless systems for smart transportation, smart homes, and smart cities will result in the proliferation of wearable devices, mobile sensors, and electronic tablets. Therefore, this paper proposes a centralized IRS design along with the NOMA-BF system to increase the number of supportable users in an energy-efficient manner. The proposed centralized IRS design supports the users in each cell through multiple clusters and serves the multiple users in each cluster through one common beamformer through the NOMA principle. Although the number of supportable users increases with the NOMA-BF system, it results in NOMA user interference as well as in ICI. Therefore the proper interference management algorithms are essential to mitigate the degrading effects.

2) *Interference management:* It is very vital to manage the interference in the IRS-enabled NOMA-BF system. This paper exploits zero-forcing beamforming along with an efficient user clustering algorithm to degrade the effects of ICI. The user clustering is based on maximum correlation and channel gain difference among users. The effect of the number of antennas at BS and passive elements at IRS on ICI is analyzed. Subsequently, the NOMA user interference is handled through a low-complexity energy-efficient power allocation algorithm that computes PAC of NOMA users in each cluster through simplified closed-form expression.

3) *Geometric channel model:* The analysis of the proposed NOMA-BF system for IRS-assisted communications is done under the consideration of a more practical geometric channel model. In the considered geometric model, the channel gains are modelled as rician fading, whose line-of-sight (LoS) component is presented by the array response of uniform linear array (ULA) of BS and IRS while the elements of the non-line-of-sight (NLoS) component are modelled as independently and identically distributed (i.i.d) complex Gaussian random variables with zero mean and unit variance.

4) *Low complexity:* The proposed energy-efficient alternating optimization algorithm provides sub-optimal EE performance for IRS aided NOMA-BF systems in very low computational complexity. The detailed complexity analysis of the proposed algorithm is presented in Section III. The performance of the proposed algorithm is analyzed through numerical Monte Carlo simulations and is compared with the benchmark algorithm. From obtained results, it is observed that the proposed algorithm can achieve higher EE performance with affordable computational complexity for practical implementations.

The main notations in this manuscript are listed as follows: The lowercase, boldface lowercase, and boldface uppercase letters, e.g., h, $\mathbf{h}$, and $\mathbf{H}$, denote a scalar, vector, and matrix, respectively.
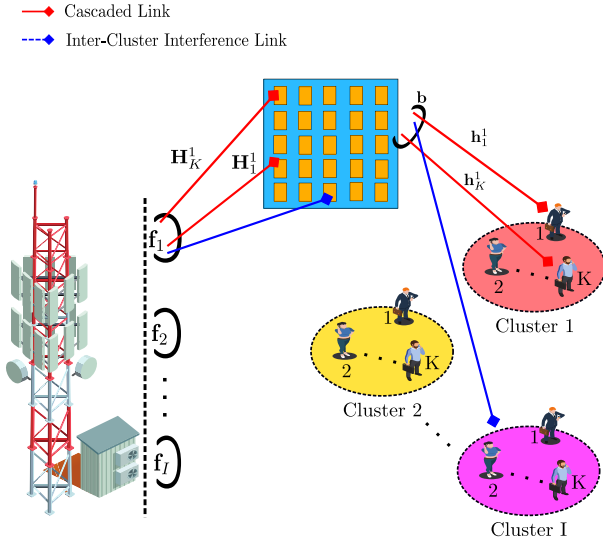
Fig. 1. Illustration of Channel gains in IRS-Enabled NOMA-BF vector.

II. SYSTEM MODEL AND PROBLEM FORMULATION

This work considers IRS-enabled downlink NOMA-BF system for beyond 5G wireless communications. The system is consist of one base station (BS) with M uniform linear array (ULA) antennas and IRS with N ULA reflecting elements, which is assisting downlink communications to K dead-zone single-antenna receivers in each cluster. The BS with M antennas can transmit $\mathcal{I}$ BF vectors, where each BF vector can serve two or more receivers through NOMA principles. A group of receivers supported by single BF vector through NOMA (NOMA-BF) is defined as cluster. There are I clusters in the system, which can support KI receivers. The BS transmits $\sum_{i=1}^{I} \mathbf{f}_i s_i$, where $\mathbf{f}_i$ is the NOMA BF vector and s_i is the superimposed information signal for NOMA receivers in the ith cluster. $s_i = \sum_{k=1}^{K} \sqrt{P_i \beta_{i,k}} x_{i,k}$, where $x_{i,k}$ is the information signal with $\mathbb{E}[|x_{i,k}|^2] = 1$, P_i is the transmit power of ith cluster and $\beta_{i,k}$ is the PAC of kth NOMA receiver ($r_{i,k}$). Let, $\mathbf{B} = diag(b_1, b_2, \ldots, b_n)$ denotes the passive beamforming matrix of IRS, where b_n is the reflection coefficient of the nth element of IRS. $b_n = \beta_n e^{j\theta_n}$ where β_n is the amplitude and θ_n is the phase shift of the reflection coefficient of IRS. In this system, the channel gains from the BS to IRS and from IRS to $r_{i,k}$ are modeled as rician fading, respectively, as follow

$$\overline{\mathbf{H}}_k^i = \sqrt{\frac{\delta}{1+\delta}} \mathbf{H}_k^{i\,LoS} + \sqrt{\frac{1}{1+\delta}} \mathbf{H}_k^{i\,NLoS}, \quad (1)$$

and

$$\overline{\mathbf{h}}_k^i = \sqrt{\frac{\epsilon}{1+\epsilon}} \mathbf{h}_k^{i\,LoS} + \sqrt{\frac{1}{1+\epsilon}} \mathbf{h}_k^{i\,NLoS}, \quad (2)$$

where $\mathbf{H}_k^{i\,LoS} \in \mathbb{C}^{N \times M}$ and $\mathbf{h}_k^{i\,LoS} \in \mathbb{C}^{N \times 1}$ are the line-of-sight (LoS) component of BS to IRS and from IRS to $r_{i,k}$ link, respectively. While $\mathbf{H}_k^{i\,NLoS} \in \mathbb{C}^{N \times M}$ and $\mathbf{h}_k^{i\,NLoS} \in \mathbb{C}^{N \times 1}$ are the non-line-of-sight (NLoS) component of BS to IRS and from IRS to $r_{i,k}$ link, respectively. δ is the Rician factor of BS to IRS link while ϵ is the Rician factor of IRS to $r_{i,k}$

link. The LoS component $\mathbf{H}_k^{i\,LoS}$ and $\mathbf{h}_k^{i\,LoS}$ depends upon the array response of ULA and can be given as follows

$$\mathbf{H}_k^{i\,LoS} = A^H(\theta^{AoA}) A(\phi_{BS}^{AoD}), \quad (3)$$

and

$$\mathbf{h}_k^{i\,LoS} = A(\phi_{IRS}^{AoD}), \quad (4)$$

where $A(\theta^{AoA})$ is the array response vector of ULA for angle of arrival (AoA) at the IRS, $A(\phi_{BS}^{AoD})$ is the array response vector of ULA for angle of departure (AoD) at BS, and $A(\phi_{IRS}^{AoD})$ is the array response of ULA for AoD at IRS. The array response of $\mathcal{E}$ elements ULA can be presented as

$$A(\Theta) = \left[1, e^{-j2\pi \frac{d}{\lambda} \sin \Theta}, \ldots, e^{-j2\pi(\mathcal{E}-1)\frac{d}{\lambda} \sin \Theta} \right], \quad (5)$$

where Θ can be AoA or AoD of the signal. d and λ are the element spacing and carrier wavelength. Each element of the NLoS components $\mathbf{H}_k^{i\,NLoS} \in \mathbb{C}^{N \times M}$ and $\mathbf{h}_k^{i\,NLoS} \in \mathbb{C}^{N \times 1}$ are independently and identically distributed (i.i.d) complex Gaussian random variables with zero mean and unit variance. Therefore, the channel gain of BS to IRS and IRS to $r_{i,k}$ link can be given as

$$\mathbf{H}_k^i = \sqrt{L_0 \left(\frac{d_{B,R}}{d_0} \right)^{-\alpha_{B,R}}} \overline{\mathbf{H}}_k^i, \quad (6)$$

and

$$\mathbf{h}_k^i = \sqrt{L_0 \left(\frac{d_{R,U}^k}{d_0} \right)^{-\alpha_{R,U}^k}} \overline{\mathbf{h}}_k^i, \quad (7)$$

where L_0 denotes the path loss at the reference distance $d_0 = 1(m)$ [25], $d_{B,R}$ is the distance from the BS to the IRS, and $d_{R,U}^k$ is the distance from the IRS to the $r_{i,k}$. $\alpha_{B,R}$ and $\alpha_{R,U}^k$ are the path-loss exponents. The illustration of the whole system model is shown in Fig. 2 while the illustration for channel gains in IRS-enabled NOMA-BF system is presented in Fig. 1. Thus the received signal at receiver $r_{i,k}$ is given by

$$y_{i,k} = \left(\mathbf{h}_k^{i\,H} \mathbf{B} \mathbf{H}_k^i \right) \mathbf{f}_i s_i + \left(\mathbf{h}_k^{i\,H} \mathbf{B} \mathbf{H}_k^i \right) \sum_{\substack{j=1 \\ j \neq i}}^{I} \mathbf{f}_j s_j + n_{i,k}, \quad (8)$$

where $n_{i,k}$ is the AWGN with zero mean and variance (σ^2). Let, $\mathbf{b} = [b_1, b_2, \ldots, b_n]^T \in \mathbb{C}^{N \times 1}$ is the vector containing diagnol elements of matrix $\mathbf{B}$. Then Eq. (8) can be written as [26]

$$y_{i,k} = \left(\mathbf{b}^H \mathbf{W}_{i,k} \right) \mathbf{f}_i s_i + \left(\mathbf{b}^H \mathbf{W}_{i,k} \right) \sum_{\substack{j=1 \\ j \neq i}}^{I} \mathbf{f}_j s_j + n_{i,k}, \quad (9)$$

where $\mathbf{W}_{i,k}$ is the cascaded channel matrix from the BS to $r_{i,k}$ through the IRS and is presented as follow

$$\mathbf{W}_{i,k} = diag\left(\mathbf{h}_k^{i\,H} \right) \mathbf{H}_k^i. \quad (10)$$
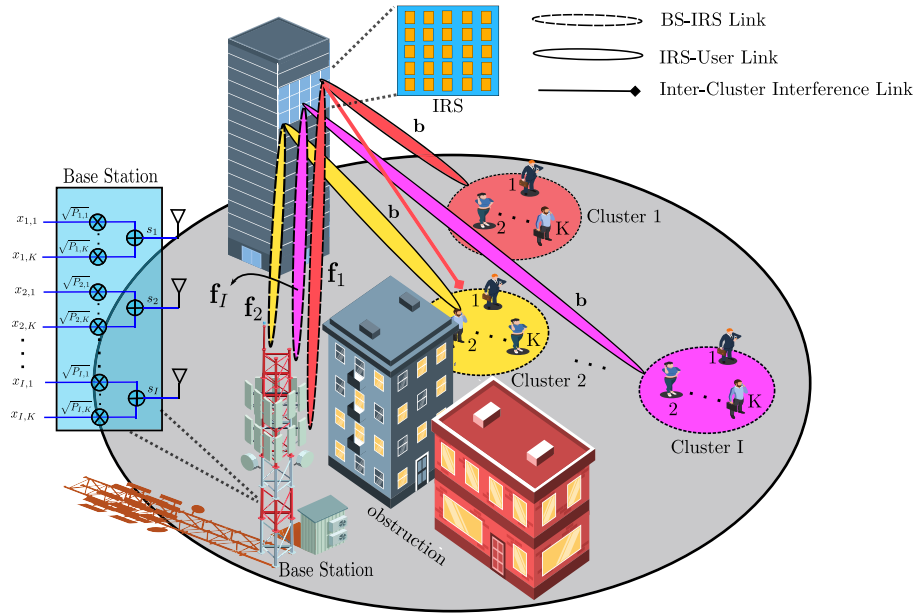
Fig. 2. Illustration of System model.

As $s_i = \sum_{k=1}^{K} \sqrt{P_i \beta_{i,k}} x_{i,k}$, Inserting it in Eq. (9) results in

$$y_{i,k} = \underbrace{\mathbf{u}_{i,k}\mathbf{f}_i\left(\sqrt{P_i\beta_{i,k}}x_{i,k}\right)}_{\text{desired signal}} + \underbrace{\mathbf{u}_{i,k}\mathbf{f}_i\sum_{\substack{l=1\\l\neq k}}^{K}\left(\sqrt{P_i\beta_{i,l}}x_{i,l}\right)}_{\text{NOMA user interference}}$$

$$+ \underbrace{\sum_{\substack{j=1\\j\neq i}}^{I}\mathbf{u}_{i,k}\mathbf{f}_j\left(\sum_{k=1}^{K}\sqrt{P_j\beta_{j,k}}x_{j,k}\right)}_{\text{Inter-cluster Interference}} + \underbrace{n_{i,k}}_{\text{noise}}, \quad (11)$$

where

$$\mathbf{u}_{i,k} = \mathbf{b}^H \mathbf{W}_{i,k}. \quad (12)$$

Without loss of generality, the channel gain of the receivers can be sorted as $||\mathbf{u}_{i,k+1}||^2 \geq ||\mathbf{u}_{i,k}||^2$. Following the consider channel order, the received SINR of $r_{i,k}$ after SIC is as follow is given as

$$\gamma_{i,k} = \frac{P_i\beta_{i,k}|\mathbf{u}_{i,k}\mathbf{f}_i|^2}{P_i\sum_{l=k+1}^{K}\beta_{i,l}|\mathbf{u}_{i,k}\mathbf{f}_i|^2 + \Psi_i + \sigma^2}, \quad (13)$$

where Ψ_i denotes ICI for i^{th} cluster and is given as follow

$$\Psi_i = \sum_{\substack{j=1\\j\neq i}}^{I}|\mathbf{u}_{i,k}\mathbf{f}_j|^2\left(\sum_{k=1}^{K}P_j\beta_{j,k}\right). \quad (14)$$

Then, the achievable rate of $r_{i,k}$ can be written as

$$R_{i,k} = BW\log_2\left(1 + \gamma_{i,k}\right). \quad (15)$$

Accordingly, the sum-rate of the each cluster is obtained as

$$R_i = \sum_{k=1}^{K}R_{i,k}. \quad (16)$$

and its corresponding power consumption is

$$P_{i,T} = \|\mathbf{f}_i\|^2 P_i \sum_{k=1}^{K}\beta_{i,k} + P_c, \quad (17)$$

where P_c is the circuit power consumption. The objective is to maximize the energy efficiency (EE) of the IRS aided NOMA-BF system through the optimization of the active beamforming and PAC of users at the BS and reflection coefficients vector of IRS for all receivers. Therefore, the energy efficiency of the system is formulated as the ratio of the sum-rate of the system to the total power consumption of the system [9] as follow

$$EE = \sum_{i=1}^{I}\frac{R_i}{P_{i,T}}, \quad (18)$$

From Eq. (11), it can be observed that sharing a BF vector through NOMA principles lead to ICI as well as NOMA user interference. Therefore, to mitigate all kinds of interferences and improve energy efficiency, this paper exploits zero-forcing beamforming and an efficient clustering algorithm for mitigation of ICI and power allocation algorithm to reduce NOMA user interference. Additionally, an energy-efficient passive beamforming algorithm for IRS is also presented that further enhance the EE of the proposed IRS aided NOMA-BF system. Under the QoS requirements of NOMA receivers, power constraint for efficient SIC implementation [27], transmit power constraint at BS and reflection coefficients constraint at IRS, the optimization problem for the proposed system can be expressed as follows

$$\max_{\boldsymbol{\beta},\mathbf{f}_i,\mathbf{b}} EE = \max_{\boldsymbol{\beta},\mathbf{f}_i,\mathbf{b}}\sum_{i=1}^{I}\frac{R_i}{P_{i,T}} \quad (19a)$$

$$s.t. \quad \gamma_{i,k} \geq \gamma_{i,k}^{\min}, \forall k, i, \quad (19b)$$

$$\|\mathbf{f}_i\|^2 P_i \beta_{i,k} |\mathbf{u}_{i,k+1}|^2 - \|\mathbf{f}_i\|^2 \sum_{l=k+1}^{K} P_i \beta_{i,l} |\mathbf{u}_{i,k+1}|^2 \geq P_g,$$
$$k = \{1, 2, \ldots, K-1\}, \forall i, \tag{19c}$$

$$\|\mathbf{f}_i\|^2 P_i \sum_{k=1}^{K} \beta_{i,k} \leq P_{\max}, \forall k, i, \tag{19d}$$

$$|b_n| = 1, \forall n, \tag{19e}$$

where EE is the energy efficiency and $\boldsymbol{\beta} = \{\beta_{i,1}, \beta_{i,2}, \ldots, \beta_{i,K}\}$ is the vector of PAC of NOMA receivers. Constraint (19b) is the QoS requirement constraint of the receivers while constraint (19c) is power constraint for efficient SIC implementation in NOMA-BF cluster and P_g is the minimum power gap required to differentiate between the information to be decoded and the remaining non-decoded information. The constraint (19d) limits the transmit power of BS to P_{max}. The constraint (19e) is the reflection coefficient constraint of the IRS.

III. THE SOLUTION OF FORMULATED PROBLEM

The EE maximization problem defined in Eq. (19) is a non-concave function, which is coupled with optimization variables such as beamforming vectors, PAC of users and IRS reflection coefficients. Thus it is very difficult to tackle it directly. To cope with this challenging problem, this work proposes a novel alternating optimization iterative algorithm. The proposed algorithm deals with the optimization problem in two stages. In the first stage, it exploits zero-forcing beamforming and optimizes the PAC of users through the fix reflection coefficient of IRS while in the 2nd stage it computes the optimal reflection coefficients of IRS with optimal active beamformers and PAC of users obtained in stage 1.

A. Stage 1: Optimization of Beamforming and PAC of the Users

For the given reflection coefficients of IRS, the optimization problem in (19) can be simplified to a subproblem of active beamforming design along with PAC of users as

$$\max_{\boldsymbol{\beta}, \mathbf{f}_i} \quad EE = \max_{\boldsymbol{\beta}, \mathbf{f}_i} \sum_{i=1}^{I} \frac{R_i}{P_{i,T}} \tag{20a}$$

$$s.t. \quad (19b), (19c), \text{ and } (19d). \tag{20b}$$

The above optimization problem has a non-concave objective function with its non-convex constraint set. Therefore, it is difficult to solve this non-convex optimization problem. For its efficient solution, first, we explored zero-forcing (ZF) beamforming, which nulls the ICI at the NOMA-BF user, whose channel gain is used to generate the beamforming vector of the Ith cluster. However, the other NOMA users in the same cluster do receive the ICI. The beamforming vectors of the clusters are generated through the channels of highest channel gain receivers as $\mathbf{U}_i = [\mathbf{u}_{1,K}, \ldots, \mathbf{u}_{i-1,K}, \mathbf{u}_{i+1,K} \ldots, \mathbf{u}_{I,K}]$. ZF beamforming will induce ZF constraint for the optimization problem defined in (20) as follows

$$\mathbf{U}_i^H \mathbf{f}_i = 0, \forall i. \tag{21}$$

Now the optimization problem in Eq. (20) can be reformulated by exploiting the problem with ZF constraint and $\|\mathbf{f}_i\|^2 = 1$, then, it can be represented as follow

$$\max_{\boldsymbol{\beta}, \mathbf{f}_i} \quad EE = \max_{\boldsymbol{\beta}, \mathbf{f}_i} \sum_{i=1}^{I} \frac{R_i}{P_{i,T}} \tag{22a}$$

$$s.t. \quad (19b), (19c), \text{ and } (19d) \tag{22b}$$

$$\mathbf{U}_i^H \mathbf{f}_i = 0, \forall i, \tag{22c}$$

$$\|\mathbf{f}_i\|^2 = 1, \forall i, \tag{22d}$$

According to [28, preposition 5.1], the optimal solution of $\mathbf{f}_i$ for problem (22) results in

$$\mathbf{f}_i = \frac{\mathbf{Q}_i \mathbf{Q}_i^H \mathbf{u}_{i,K}}{\|\mathbf{Q}_i \mathbf{Q}_i^H \mathbf{u}_{i,K}\|^2}, \tag{23}$$

where $\mathbf{Q}_i$ is the orthogonal basis of the null space of $\mathbf{U}_i^H$. It can be observed that the objective function (22a) increases with the increase in the values of the terms $|\mathbf{u}_{i,k}\mathbf{f}_i|^2$ and with the decrease in the term of ICI. The beamforming vectors for clusters are generated through the channel of the highest channel gain users, therefore the optimal value of $\mathbf{f}_i$ computed through Eq. (23) will maximize the $|\mathbf{u}_{i,k}\mathbf{f}_i|^2$ term for highest channel gain user and will also null its ICI term. However, for the other users in the cluster, we still need to implement an efficient user clustering algorithm for ICI mitigation. For the proposed IRS-assisted NOMA-BF system, it is observed that ICI depends on correlation and gain-difference among the channel of users in a cluster. It exploits Zero-forcing beamforming and beamforming vectors of the clusters are generated through the channel gains of the highest channel gain users. Therefore, a higher correlation of the channels of the other users with the highest channel gain user in the cluster reduces ICI. Besides, if the channel gain difference among the users is maximum, it leads to a higher power difference among the received signals of the users in the same cluster. In practice, it fosters the SIC implementation because the power difference among the user signals needs to be higher when implementing SIC in the downlink. Therefore, the proposed clustering algorithm chooses the highest channel gain correlation user in the cluster under the maximum channel gain difference. After obtaining the optimal active beamformers, and implementing the efficient user clustering as presented in Algorithm 1, the optimization problem in (22) can be simplified as follow,

$$\max_{\boldsymbol{\beta}} \quad EE = \max_{\boldsymbol{\beta}} \sum_{i=1}^{I} \frac{R_i}{P_{i,T}} \tag{24a}$$

$$s.t. \quad \gamma_{i,k} \geq \gamma_{k,\min}^i, \forall k, i, \tag{24b}$$

$$P_i \beta_{i,k} |\mathbf{u}_{i,k+1}|^2 - \sum_{l=k+1}^{K} P_i \beta_{l,k} |\mathbf{u}_{i,k+1}|^2 \geq P_g \forall k, i, \tag{24c}$$

$$P_i \sum_{k=1}^{K} \beta_{i,k} \leq P_{\max}, \forall k, i, \tag{24d}$$

The objective function of the above optimization problem has a non-linear fractional form, which is non-convex for the optimization variable $\beta_{i,k}$. Therefore, logarithmic approximation [29] is adopted to tackle this challenging problem.

Algorithm 1 User-Clustering for IRS-Enabled NOMA-BF System for Mitigation of ICI

1: **Initialize:** Total number of users in a cell $\mathcal{V}$, number of users per cluster K, number of clusters $\mathcal{I}$, x=1, i=1 and threshold Δ where $(0 \geq \Delta \leq 1)$.

2: Generate channel gain of all users for IRS-enabled NOMA-BF system, i.e., $G = [\mathbf{u}_1, \mathbf{u}_2, \ldots, \mathbf{u}_v, \ldots, \mathbf{u}_V]$. Where $\mathbf{u}_v = \mathbf{b}_v^H \mathbf{W}_v$ and $\mathbf{W}_v = diag(\mathbf{h}_v{}^H)\mathbf{H}_v$

3: **Stage:1** Compute the channel gain difference of user with all other users in the cell under the pre-defined correlation threshold. The channel gain difference of all users with respect to others should be computed as follow,

4: **while** $x \leq \mathcal{V}$ **do**

5:    **for** y=x+1:$\mathcal{V}$ **do**

6:       $C(x, y) = \frac{|\mathbf{u}_x^H \mathbf{u}_y|}{|\mathbf{u}_x^H||\mathbf{u}_y|}$

7:       **if** $C(x, y) > \Delta$ **then**

8:          $D(x, y) = ||u_x||^2 - ||u_y||^2$

9:       **else**

10:          $D(x, y) = 0$

11:       **end if**

12:    **end for**

13:    $x = x + 1$

14: **end while**

15: **Output:** A matrix **D**.

16: **Stage:2** User grouping

17: **while** $i \leq \mathcal{I}$ **do**

18:    $Cluster_i = max(\mathbf{D})$ selects the users which has highest channel gain difference among them under the predefined channel correlation threhold.

19:    Remove the selected users channel gain difference entries with all other users from **D**.

20:    $i = i + 1$

21: **end while**

22: **Output:** $\mathcal{I}$ Clusters.

This successive convex approximation (SCA) approximates the sum-rates expression in each iteration as follow

$$\zeta \log_2(\gamma) + \Omega \leq \log_2(1 + \gamma), \tag{25}$$

where $\zeta = \frac{\gamma_0}{1+\gamma_0}$ and $\Omega = \log_2(1+\gamma_0) - \frac{\gamma_0}{1+\gamma_0}\log_2(\gamma_0)$. When $\gamma = \gamma_0$, the bound becomes tight. Through lower bound of inequality in Eq. (25), the sum-rate of IRS NOMA-BF system is presented as

$$\overline{R}_i = \sum_{k=1}^{K} BW\big(\zeta_{i,k} \log_2(\gamma_{i,k}) + \Omega_{i,k}\big), \tag{26}$$

where

$$\zeta_{i,k} = \frac{\gamma_{i,k}}{1 + \gamma_{i,k}}, \tag{27}$$

and

$$\Omega_{i,k} = \log_2\big(1 + \gamma_{i,k}\big) - \frac{\gamma_{i,k}}{1 + \gamma_{i,k}}\log_2\big(\gamma_{i,k}\big). \tag{28}$$

Based on the above logarithmic approximation, the optimization problem in Eq. (24) can be rewritten as

$$\max_{\boldsymbol{\beta}} \quad EE = \max_{\boldsymbol{\beta}} \sum_{i=1}^{I} \frac{\overline{R}_i}{P_{i,T}} \tag{29a}$$

$$s.t. \; (24\,\text{b}), (24\,\text{c}), \; \text{and} \; (24\,\text{d}). \tag{29b}$$

Now, the above problem can be solved in an affordable complexity through Dinkelbach's algorithm [30], which transforms the fractional objective function in Eq. (29a) to parametric form as

$$\max_{\boldsymbol{\beta}} EE = \max_{\boldsymbol{\beta}} \; \sum_{i=1}^{I} F(\rho_i) = \max_{\boldsymbol{\beta}} \sum_{i=1}^{I} \overline{R}_i - \rho_i P_{i,T}, \tag{30}$$

where, ρ_i presents the maximum EE of ith cluster. The computation of roots of $F(\rho_i)$ is analogous to the solution of the objective function in Eq. (29a) [31]. $F(\rho_i)$ is convex for ρ_i because $F(\rho_i)$ is negative when ρ_i approaches infinity, while $F(\rho_i)$ is positive when ρ_i approaches minus infinity. The convex problem in Eq. (30) is solved by employing the special case of Lagrangian relaxation, which is known as dual decomposition. The Lagrangian function of the optimization problem in (30) presented as follow

$$\mathcal{L}(\boldsymbol{\beta}, \alpha_i, \boldsymbol{\varphi_i}, \boldsymbol{\Upsilon_i}) = \overline{R}_i - \rho_i P_{i,T} + \alpha_i \left(P_{max} - P_i \sum_{k=1}^{K} \beta_{i,k} \right)$$

$$+ \sum_{k=1}^{K} \varphi_{i,k}\left(\gamma_{i,k} - \gamma_{i,k}^{\min}\right) + \sum_{k=1}^{K-1} \Upsilon_{i,k}\left(P_i\beta_{i,k}|\mathbf{u}_{i,k+1}|^2 \right.$$

$$\left. - \sum_{l=k+1}^{K} P_i\beta_{i,l}|\mathbf{u}_{i,k+1}|^2 - P_g \right), \tag{31}$$

where α, $\boldsymbol{\varphi_i} = \{\varphi_{i,1}, \varphi_{i,2}, \ldots, \varphi_{i,K}\}$, and $\boldsymbol{\Upsilon_i} = \{\Upsilon_{i,1}, \Upsilon_{i,2}, \ldots, \Upsilon_{i,K}\}$ are the Lagrange multipliers. Constraints are KKT conditions for optimizing the power allocation of NOMA-BF users.

Lemma 1: The closed-form solution of optimal PAC of NOMA-BF user can be expressed as

$$\beta_{i,k} = \frac{BW\zeta_{i,k}}{\ln 2\big((\rho_i + \alpha_i)P_i - \Gamma_{i,k}\big) + \sum_{z=1}^{k-1} \Pi\big(\beta_{i,z}\big)}, \tag{32}$$

where

$$\Gamma_{i,k} = \varphi_{i,k} P_i|\mathbf{u}_{i,k}\mathbf{f}_i|^2 - \Upsilon_{i,k}|\mathbf{u}_{i,k+1}|^2, \tag{33}$$

and

$$\Pi(\beta_{i,z}) = \left(\frac{BW\zeta_{i,z}}{\beta_{i,z}} \right)\gamma_{i,z} + \varphi_{i,z}P_i|\mathbf{u}_{i,z}\mathbf{f}_i|^2\gamma_{i,z}^{\min} + \Upsilon_{i,z}|\mathbf{u}_{i,z+1}|^2. \tag{34}$$

Proof: Please, refer to the Appendix. ∎

Given the optimal PAC policy in Eq. (32), the primal problem's dual variables can be computed and updated iteratively by using the sub-gradient method.

$$\alpha_i(iter + 1) = \left[\alpha_i(iter) - \omega_1(iter)\left(P_{max} - P_i \sum_{k=1}^{K} \beta_{i,k} \right) \right]^+, \tag{35}$$

$$\varphi_{i,k}(iter + 1) = \left[\varphi_{i,k}(iter) - \omega_2(iter)\left(P_i\beta_{i,k}|\mathbf{u}_{i,k}\mathbf{f}_i|^2 \right.\right.$$

$$\left.\left. - \gamma_{i,k}^{\min}\left(P_i \sum_{l=k+1}^{K} \beta_{i,l}|\mathbf{u}_{i,k}\mathbf{f}_i|^2 + \Psi_i + \sigma^2 \right) \right) \right]^+, \tag{36}$$

$$\Upsilon_{i,k}(iter+1) = \left[\Upsilon_{i,k}(iter) - \omega_3(iter)\left(P_i\beta_{i,k}|\mathbf{u}_{i,k+1}|^2\right.\right.$$
$$\left.\left. - \sum_{l=k+1}^{K} P_i\beta_{i,l}|\mathbf{u}_{i,k+1}|^2 - P_g\right)\right]^+, \quad (37)$$

where *iter* is used for iteration index. ω_1, ω_2, and ω_3 present positive step sizes. It is important to use the appropriate step sizes for the convergence to an optimal solution.

B. Stage 2: Efficient Reflection Coefficients of IRS

For the optimal beamformers and PAC of NOMA-BF users computed at stage 1, the efficient reflection coefficient of IRS can be obtained through the following subproblem of optimization

$$\max_{\boldsymbol{b}} \quad EE = \max_{\boldsymbol{b}} \sum_{i=1}^{I} \overline{R}_i - \rho P_{i,T} \quad (38a)$$
$$s.t. \ \ \gamma_{i,k} \geq \gamma_{i,k}^{\min}, \forall k,i \quad (38b)$$
$$|b_n| = 1, \forall n, \quad (38c)$$

For the efficient solution, it is important to first transform the above formulated problem into tractable form. Let $\boldsymbol{\omega}_{i,k} = \mathbf{W}_{i,k}\mathbf{f}_i$ in Eq. (9), the received SINR of $r_{i,k}$ can be represented as

$$\gamma_{i,k} = \frac{P_i\beta_{i,k}|\mathbf{b}^H\boldsymbol{\omega}_{i,k}|^2}{P_i\sum_{l=k+1}^{K}\beta_{i,l}|\mathbf{b}^H\boldsymbol{\omega}_{i,k}|^2 + \Psi_i + \sigma^2}, \quad (39)$$

where, Ψ_i will become as follow

$$\Psi_i = \sum_{\substack{j=1 \\ j\neq i}}^{I} |\mathbf{b}^H\boldsymbol{\omega}_{j,k}|^2\left(P_j\sum_{k=1}^{K}\beta_{j,k}\right). \quad (40)$$

Then,

$$\overline{R}_i^* = \sum_{k=1}^{K} BW\left(\zeta_{i,k}\log_2\left(\gamma_{i,k}^*\right) + \Omega_{i,k}\right), \quad (41)$$

$$\overline{R}_i^* = \sum_{k=1}^{K} BW\left(\zeta_{i,k}\left[\log_2\left(P_i\beta_{i,k}|\mathbf{b}^H\boldsymbol{\omega}_{i,k}|^2\right)\right.\right.$$
$$\left. - \log_2\left(P_i\sum_{l=k+1}^{K}\beta_{i,l}|\mathbf{b}^H\boldsymbol{\omega}_{i,k}|^2 + \Psi_i + \sigma^2\right)\right]$$
$$\left. + \Omega_{i,k}\right), \quad (42)$$

Let $\mathbf{B} = \mathbf{b}\mathbf{b}^H$ and $\boldsymbol{W_{i,k}} = \boldsymbol{\omega}_{i,k}\boldsymbol{\omega}_{i,k}^H$, where $\mathbf{B} \succeq 0$ and rank $(\mathbf{B}) = 1$, $\boldsymbol{W_{i,k}} \succeq 0$ and rank $(\boldsymbol{W_{i,k}}) = 1$, then $\overline{R}_i^*$ can be expressed as

$$\overline{R}_i^* = \sum_{k=1}^{K} BW\left(\zeta_{i,k}\left[\log_2\left(P_i\beta_{i,k}tr(\mathbf{B}\boldsymbol{W_{i,k}})\right)\right.\right.$$
$$\left. - \log_2\left(P_i\sum_{l=k+1}^{K}\beta_{i,l}tr(\mathbf{B}\boldsymbol{W_{i,k}}) + \Psi_i + \sigma^2\right)\right] + \Omega_{i,k}\right), \quad (43)$$

Furthermore, $\overline{R}_i^*$ can be presented as a function of $\mathbf{B}$ as

$$\overline{R}_i^* = \sum_{k=1}^{K} BW\left(\zeta_{i,k}[f_1(\mathbf{B}) - f_2(\mathbf{B})] + \Omega_{i,k}\right), \quad (44)$$

where,

$$f_1(\mathbf{B}) = \log_2\left(P_i\beta_{i,k}tr\left(\mathbf{B}\boldsymbol{W_{i,k}}\right)\right),$$
$$f_2(\mathbf{B}) = \log_2\left(P_i\sum_{l=k+1}^{K}\beta_{i,l}tr\left(\mathbf{B}\boldsymbol{W_{i,k}}\right) + \Psi_i + \sigma^2\right), (45)$$

It can be observed that $\overline{R}_i^*$ in Eq. (44) is still not a concave function because it is the difference between two concave functions. Therefore, optimization problem in Eq. (38) is not a convex optimization problem. This non-convex optimization problem is transformed into a convex problem by employing low complexity suboptimal technique based on DC programming. In this technique, instead of $f_2(\mathbf{B})$, we substitute its first-order linear approximation as follows

$$f_2(\mathbf{B}) \leq f_2\left(\mathbf{B}^{(t)}\right) + tr\left(\left(f_2'\left(\mathbf{B}^{(t)}\right)\right)^H\left(\mathbf{B} - \mathbf{B}^{(t)}\right)\right),$$
$$\triangleq \overline{f_2(\mathbf{B})} \quad (46)$$

where $\mathbf{B}^{(t)}$ is the value of $\mathbf{B}$ at t^{th} iteration and $f_2'(\mathbf{B}^{(t)})$ is the first derivative of $f_2(\mathbf{B})$ at t^{th} iteration, which can be computed as follows

$$f_2'\left(\mathbf{B}^{(t)}\right) = \frac{\sum_{l=k+1}^{K} P_i\beta_{i,l}\boldsymbol{W_{i,k}}^H}{\left(P_i\sum_{l=k+1}^{K}\beta_{i,l}tr(\mathbf{B}\boldsymbol{W_{i,k}}) + \Psi_i + \sigma^2\right)\ln(2)} \quad (47)$$

Therefore, $\overline{R}_i^*$ can approximately transformed into the following form

$$\overline{R}_i^* = \sum_{k=1}^{K} BW\left(\zeta_{i,k}\left[f_1(\mathbf{B}) - \overline{f_2(\mathbf{B})}\right] + \Omega_{i,k}\right), \quad (48)$$

Based on the above computations and approximation, the optimization problem in Eq. (38) can be rewritten as

$$\max_{\boldsymbol{b}} \quad EE = \max_{\boldsymbol{b}} \sum_{i=1}^{I}\sum_{k=1}^{K} BW\left(\zeta_{i,k}\left[f_1(\mathbf{B}) - \overline{f_2(\mathbf{B})}\right] + \Omega_{i,k}\right)$$
$$-\rho P_{i,T} \quad (49a)$$
$$s.t. \ \ P_i\beta_{i,k}tr\left(\mathbf{B}\boldsymbol{W_{i,k}}\right) \geq \gamma_{i,k}^{\min}$$
$$\times \left(P_i\sum_{l=k+1}^{K}\beta_{i,l}tr\left(\mathbf{B}\boldsymbol{W_{i,k}}\right) + \Psi_i + \sigma^2\right), \forall k,i \ (49b)$$
$$diag(\mathbf{B}) \leq 1, \quad (49c)$$
$$\mathbf{B} \succeq 0, \quad (49d)$$
$$rank(\mathbf{B}) = 1, \quad (49e)$$

The rank one constraint in the above optimization problem is non-convex which is first transformed in the form of difference of two convex functions as follows

$$rank(\mathbf{B}) = 1 \Leftrightarrow tr(\mathbf{B}) - ||\mathbf{B}||_2 = 0, \quad (50)$$

where $tr(\mathbf{B}) = \sum_{n=1}^{N} \lambda_n$ and λ_n presents n^{th} largest singular value of $\mathbf{B}$. $||\mathbf{B}||_2$ is the spectral norm of matrix $\mathbf{B}$. The transformed rank one constraint is still non-convex, therefore SCA is exploited to replace $||\mathbf{B}||_2$ with its first order taylor approximation to obtain its lower bound as follows

$$||\mathbf{B}||_2 \geq ||\mathbf{B}^{(t)}||_2 tr\left(\varkappa_{max}^{(t)} \varkappa_{max}^{(t)}{}^{H} \left(\mathbf{B} - \mathbf{B}^{(t)} \right) \right),$$
$$\triangleq \overline{||\mathbf{B}||_2}, \tag{51}$$

where $\varkappa_{max}^{(t)}$ is the eigenvector corresponding to the largest singular value of matrix $\mathbf{B}$ in the tth iteration. Then, add the transformed rank one constraint to the objective function as a penalty term in the optimization problem presented in Eq as follow

$$\max_{\mathbf{b}} \quad EE = \max_{\mathbf{b}} \sum_{i=1}^{I} \sum_{k=1}^{K} BW \left(\zeta_{i,k} \left[f_1(\mathbf{B}) - \overline{f_2(\mathbf{B})} \right] + \Omega_{i,k} \right)$$
$$- \rho P_{i,T} - \eta \left(tr(\mathbf{B}) - \overline{||\mathbf{B}||_2} \right) \tag{52a}$$
$$s.t. \quad (49\,\mathrm{b}), (49\,\mathrm{c}), \quad \mathrm{and} \quad (49\,\mathrm{d}), \tag{52b}$$

where, $\eta >> 0$ is the penalty factor of the rank one constraint. The above problem is now in the form of standard semi-definite programming (SDP) problem, which can be solved through the MOSEK optimization toolbox for MATLAB. MOSEK in each iteration solves a relaxed SDP problem through the interior point method, whose computational complexity can be given by $\mathcal{O}(N)^{3.5}$. If l is the number of iterations that are required for the ORCA algorithm to reach convergence. Then, the total computational complexity of the ORCA algorithm is $\mathcal{O}(lKIN^{3.5})$. The detailed two stage energy-efficient resource allocation for IRS-enabled NOMA-BF system is presented in Algorithm 2. The total computational complexity of Algorithm 2 is $\mathcal{O}(q(T(KI)^2 + lKIN^{3.5}))$. q is the number of iterations required for the convergence of Algorithm 2 while $T(KI)^2$ is complexity of stage 1. Where T is the number of iterations required for the convergence of stage 1, K is the total number of users in each cluster and I is the total number of clusters in the system.

IV. RESULTS AND DISCUSSION

This section presents the simulation results of our proposed energy efficient IRS NOMA-BF algorithm for extremely overloaded 6G wireless communications systems. The results are obtained using Monte Carlo simulations. We compare the proposed IRS NOMA-BF approach with IRS conventional BF approach as the benchmark. The considered benchmark refers to multiuser BF systems that serve users orthogonally through BF vectors. That is each user in a cluster is supported by a single BF vector, orthogonal to the other users' channels in order to eliminate interference from other users in the cluster. In our simulations, the BS has 5 transmit BF vectors, where each BF vector can support a group of two users defined as a cluster. A total of 5 clusters are generated through our proposed clustering from 30 users which are deployed randomly around the IRS through binomial point process (BPP). The minimum distance between BS and IRS is assumed to be 30m while

---

Algorithm 2 Energy-Efficient Resource Allocation for IRS-Enabled NOMA-BF System

1: **while** not converge **do**
2: 　　**Stage 1: Optimization of Beamforming and PAC of the Users**
3: 　　**Initialization:** Initialize the PAC for each NOMA-BF user, stepsizes, dual variables, maximum iterations L_{max}, iteration index $l = 1$ and maximum tolerance δ_{max}.
4: 　　**for** $l \leq L_{max}$ **do**
5: 　　　　Compute $\overline{R}_i(l)$ by using Eq. (26)
6: 　　　　Compute $\rho_i(l) = \dfrac{\overline{R}_i(l)}{||\mathbf{f}_i||^2 P_i \sum_{k=1}^{K} \beta_{i,k} + P_c}$
7: 　　　　Update dual variables $\alpha_i(l)$, $\boldsymbol{\varphi_i}(l)$, and $\boldsymbol{\Upsilon_i}(l)$ by using Eq. (35), (36) and (37), respectively.
8: 　　　　Update the PAC vector $\boldsymbol{\beta}(l+1)$ of IRS NOMA-BF users by using equation (32)
9: 　　　　**if** $|F_i^{(l)}(\rho) - F_i^{(l-1)}(\rho)| \leq \delta_{max}$ **then**
10: 　　　　　**break;**
11: 　　　　**end if**
12: 　　**end for**
13: **Output:** Optimal $\boldsymbol{\beta}^* = \{\beta_{i,1}^*, \beta_{i,2}^*, \ldots, \beta_{i,K}^*\}$
14: 　　**Stage 2: Optimized reflection coefficients algorithm (ORCA) for IRS NOMA-BF system**
15: 　　**Problem Transformation:** Transform the IRS RC optimization problem defined in into tractable form through following steps.
16: 1) **DC programming**: Apply DC programming approch on the $\overline{R}_i^*$ using Eq. (48)
17: 2) **Rank one constraint approximation**: Transform the non-convex rank one constraint in the form of difference of two convex functions using Eq (50) and then apply SCA on it using Eq. (51).
18: 3) **Penalty function method:** Then, add the transformed rank one constraint to the objective function as a penalty term as shown in Eq. (52).
19: 　　**Problem Solution:** The tractable form is Standard SDP problem which can be solved through MOSEK optimization toolbox for MATLAB.
20: **Output:** Optimal $\mathbf{b}^*$
21: **end while**
22: **return** Optimized Beamforming, $\boldsymbol{\beta}^*$ and $\mathbf{b}^*$

---

the locations of users around IRS are modelled as binomial point process (BPP) in a circle of radius 10m. For $d_0 = 1\,(m)$, L_0 is set to -30dB. The path loss exponents are set as 2.2. The number of antennas at BS and the number of elements at IRS are mentioned with each figure. Other main simulation parameters for our setup are described in table I.

Figure 3 compares the EE of the proposed IRS NOMA-BF algorithm with IRS conventional BF as the benchmark. The comparison is done with the different number of antennas at BS versus the different number of elements at the IRS. It can be observed from the figure that the proposed algorithm performs better than the benchmark in terms of EE. Moreover, it can be noticed that a higher number of antennas at BS and a higher number of elements at IRS results in higher EE.

Figure 4 depicts the efficacy of the proposed clustering in terms of ICI reduction while Figure 5 presents its efficacy in terms of EE. It can be analyzed from the figures that proposed clustering reduces ICI and thus increases the EE of the IRS NOMA-BF system. From these figures, it can be concluded that it is very important to consider an efficient

TABLE I
SIMULATION PARAMETERS

Parameter	Value
Number of beamforming vectors	5
Number of clusters	5
Number of users per clusters	2
Users distribution around IRS	BPP
IRS radius	10m
path-loss exponent(α)	2.2
Noise power (σ^2)	-114 dBm
Transmit power of each cluster (P_i)	30 dBm
Rician factor (δ)	3 dB
Rician factor (ϵ)	3 dB
The path loss L_0 with $d_0 = 1(m)$	-30dB
Distance between IRS and BS ($d_{B,R}$)	30m
Circuit power consumption (P_c)	30 dBm
minimum SINR $\gamma_{k,min}^i$	3 dB
Fast fading	Rician fading
Pathloss model	distance dependent
Correlation threshold (Δ)	Between 0 and 1

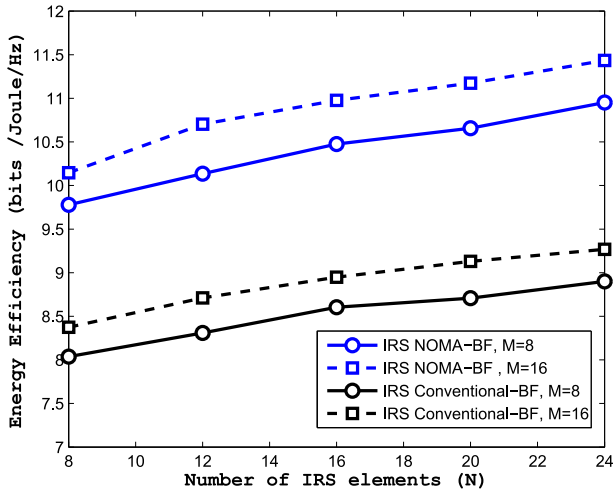Fig. 5. Energy efficiency of IRS NOMA-BF under proposed clustering and random clustering versus number of IRS elements.

Fig. 3. Energy efficiency comparison of proposed algorithm with benchmark algorithm versus number of IRS elements.

Fig. 6. Energy efficiency of proposed algorithm under different stages versus number of IRS elements.

as compared to ICI, they greatly improve the desired signal at users. Therefore, the higher number of BS antennas and IRS elements result in higher EE performance.

Figure 6 demonstrates that after efficient clustering the performance of the IRS NOMA-BF system can further be enhanced through efficient PAC of users that share the same BF vector and through efficient allocation of refection coefficients at IRS. The proposed algorithm achieves optimal EE in two stages. Stages 1 is named as optimized power allocation coefficients (OPAC) stage, which allocates efficient PAC to the users. It can be observed from the figure that OPAC attain higher EE than random allocation algorithm. The optimized reflection coefficient algorithm (ORCA) is the second stage of the proposed algorithm which additionally improve the EE of the IRS NOMA-BF system.

Our proposed alternating optimization framework for the IRS NOMA-BF system is consist of two stages, where the first stage employs the OPAC algorithm for optimal PAC of users and 2nd stage also employs an iterative algorithm for optimal RC of IRS. Therefore, it is necessary to analyze the convergence of both OPAC and ORCA algorithms. In
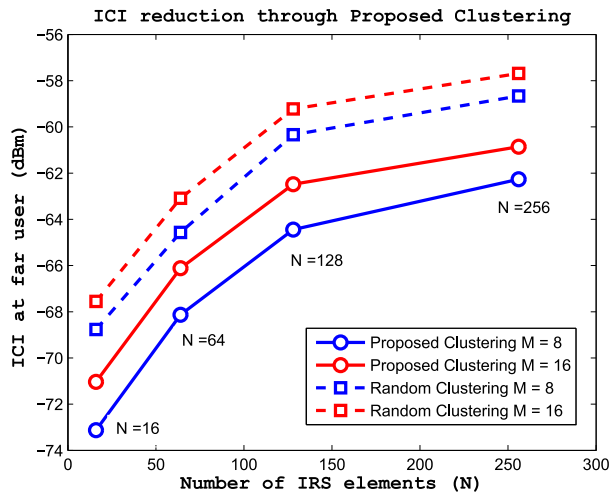

Fig. 4. ICI at far user under proposed clustering and random clustering versus number of IRS elements.

clustering algorithm among the users which shares the same beamforming vector. Besides it, the higher number of antennas at BS and higher number of elements at IRS increase ICI but
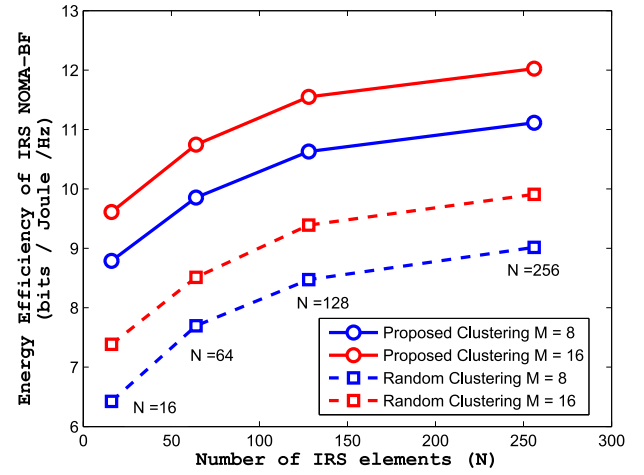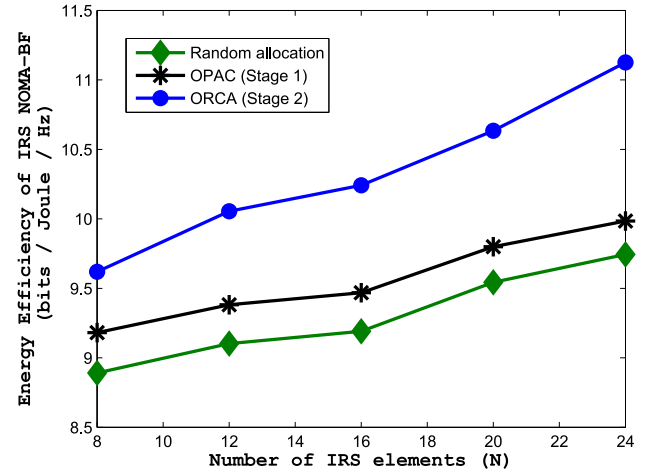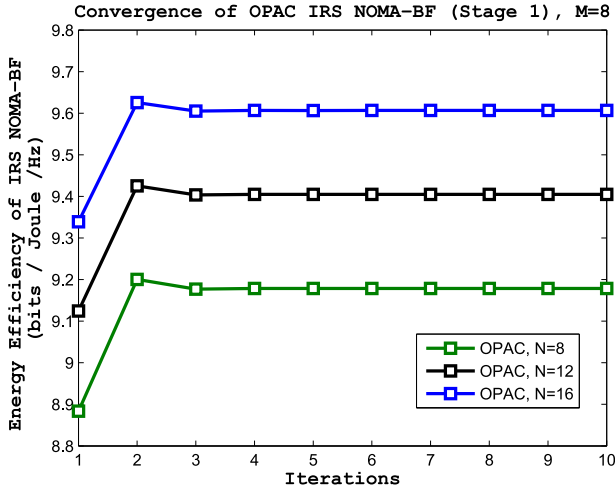
Fig. 7. Energy efficiency convergence of OPAC algorithm (Stage 1) for IRS NOMA-BF system.
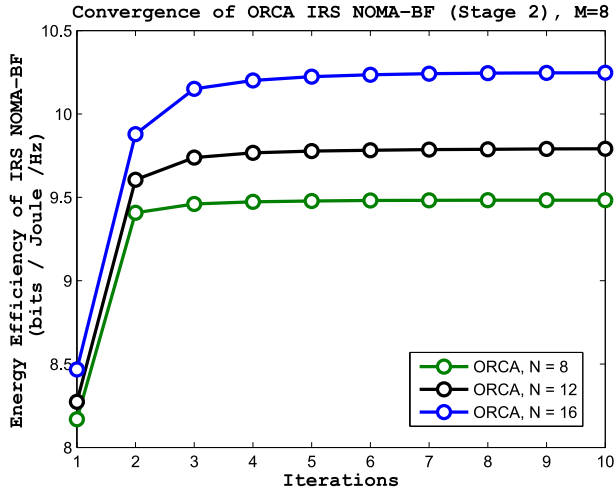

Fig. 8. Energy efficiency convergence of ORCA algorithm (Stage 2) for IRS NOMA-BF system.

Fig. 7, EE convergence of OPAC algorithm versus iterations is demonstrated with the different number of IRS elements (N). The obtained result shows that the OPAC algorithm usually converges in four iterations regardless of N. It is analyzed that N affects EE, but it has a negligible effect on the convergence of the OPAC algorithm. Similarly, in the 2nd stage ORCA algorithm achieve convergence in the 5th iteration regardless of the number of IRS elements as shown in Fig. 8.

V. CONCLUSION

A novel alternating optimization framework has been proposed to enhance the energy efficiency of IRS-assisted NOMA-BF systems for next-generation wireless communication networks. More specifically, we aim to maximize the energy efficiency of the considered IRS-assisted NOMA-BF system by optimizing the active beamforming and PAC at the source, and passive beamforming at the IRS node of the system. However, an increment in the number of supportable users with the NOMA-BF system will lead to NOMA user interference and ICI. In this regard, zero-forcing beamforming

along with an effective clustering algorithm is exploited to reduce the effect of ICI. Furthermore, a two-stage low-complexity iterative alternating optimization algorithm has been proposed for considered IRS-assisted NOMA-BF system. In the first stage, NOMA user interference is tackled by efficiently optimizing the PAC of NOMA users under the required system constraints. However, in the second stage of the proposed algorithm, passive beamforming has been optimized based on the difference-of-convex (DC) programming and successive convex approximation (SCA). Moreover, numerical simulation results depict that the proposed alternating optimization framework outperforms its counterpart by providing an efficient performance in terms of the energy efficiency of the system.

APPENDIX
DERIVATION OF OPTIMAL PAC OF NOMA-BF USERS AT THE TRANSMITTER

For efficient SIC process at receivers in each cluster, it is assumed that users are sorted according to the channel gain as $||\mathbf{u}_{i,k+1}||^2 \geq ||\mathbf{u}_{i,k}||^2$.

When $k = 1$, the optimal closed-form expression of the first user in the NOMA-BF cluster can be calculated as

$$\frac{\partial \mathcal{L}(\boldsymbol{\beta}, \alpha, \boldsymbol{\varphi}, \boldsymbol{\Upsilon})}{\partial \beta_{i,1}} = \frac{BW\zeta_{i,k}}{\ln 2\beta_{i,1}} - \rho_i P_i - \alpha_i P_i + \varphi_{i,1} P_i |\mathbf{u}_{i,1}\mathbf{f}_i|^2 + \Upsilon_{i,1} |\mathbf{u}_{i,2}|^2 = 0, \tag{53}$$

Then

$$\beta_{i,1} = \frac{BW\zeta_{i,1}}{\ln 2\big((\rho_i + \alpha_i)P_i - \Gamma_{i,1}\big)}, \tag{54}$$

where

$$\Gamma_{i,1} = \varphi_{i,1} P_i |\mathbf{u}_{i,1}\mathbf{f}_i|^2 + \Upsilon_{i,1} |\mathbf{u}_{i,2}|^2. \tag{55}$$

When $k = 2$, the optimal closed-form expression of the 2nd user in the NOMA-BF cluster can be computed as

$$\frac{\partial \mathcal{L}(\boldsymbol{\beta}, \alpha, \boldsymbol{\varphi}, \boldsymbol{\Upsilon})}{\partial \beta_{i,2}} = \left(\frac{-BW\zeta_{i,1} P_i |\mathbf{u}_{i,1}\mathbf{f}_i|^2}{\ln 2(P_i|\mathbf{u}_{i,1}\mathbf{f}_i|^2(\beta_{i,2} + \beta_{i,3}) + \Psi_i + \sigma^2)} \right)$$
$$+ \frac{BW\zeta_{i,2}}{\ln 2\beta_{i,2}} - \rho_i P_i - \alpha_i P_i - \varphi_{i,1}\gamma_{i,1}^{\min} P_i |\mathbf{u}_{i,1}\mathbf{f}_i|^2 + \varphi_{i,2} P_i |\mathbf{u}_{i,2}\mathbf{f}_i|^2$$
$$+ \Upsilon_{i,2}|\mathbf{u}_{i,3}|^2 - \Upsilon_{i,1}|\mathbf{u}_{i,2}|^2 = 0, \tag{56}$$

Then we can obtain

$$\beta_{i,2} = \frac{BW\zeta_{i,2}}{\ln 2\big((\rho_i + \alpha_i)P_i - \Gamma_{i,2}\big) + \Pi\big(\beta_{i,1}\big)}, \tag{57}$$

where

$$\Gamma_{i,2} = \varphi_{i,2} P_i |\mathbf{u}_{i,2}\mathbf{f}_i|^2 - \Upsilon_{i,2}|\mathbf{u}_{i,3}|^2, \tag{58}$$

$$\Pi\big(\beta_{i,1}\big) = \frac{BW\zeta_{i,1}}{\ln 2\beta_{i,1}}\gamma_{i,1} + \varphi_{i,1}\gamma_{i,1}^{\min} P_i |\mathbf{u}_{i,1}\mathbf{f}_i|^2 + \Upsilon_{i,1}|\mathbf{u}_{i,2}|^2. \tag{59}$$

When $k = 3$, the optimal closed-form expression of the 3rd user in the NOMA-BF cluster can be evaluated as

$$\frac{\partial \mathcal{L}(\boldsymbol{\beta}, \alpha, \boldsymbol{\varphi}, \boldsymbol{\Upsilon})}{\partial \beta_{i,3}} = \left(\frac{-BW\zeta_{i,1} P_i |\mathbf{u}_{i,1}\mathbf{f}_i|^2}{\ln 2(P_i|\mathbf{u}_{i,1}\mathbf{f}_i|^2(\beta_{i,2} + \beta_{i,3}) + \Psi_i + \sigma^2)} \right)$$
$$\left(\frac{-BW\zeta_{i,2} P_i |\mathbf{u}_{i,2}\mathbf{f}_i|^2}{\ln 2(P_i|\mathbf{u}_{i,2}\mathbf{f}_i|^2(\beta_{i,3}) + \Psi_i + \sigma^2)} \right) + \frac{BW\zeta_{i,3}}{\ln 2\beta_{i,3}} - \rho_i P_i - \alpha_i P_i$$

$$-\varphi_{i,1}\gamma_{i,1}^{\min}P_i|\mathbf{u}_{i,1}\mathbf{f}_i|^2 - \varphi_{i,2}\gamma_{i,2}^{\min}P_i|\mathbf{u}_{i,2}\mathbf{f}_i|^2 + \varphi_{i,3}P_i|\mathbf{u}_{i,3}\mathbf{f}_i|^2$$
$$-\Upsilon_{i,2}|\mathbf{u}_{i,3}|^2 - \Upsilon_{i,1}|\mathbf{u}_{i,2}|^2 = 0, \tag{60}$$

Then we have

$$\beta_{i,3} = \frac{BW\zeta_{i,3}}{\ln 2\big((\rho_i + \alpha_i)P_i - \Gamma_{i,3}\big) + \Pi\big(\beta_{i,1}\big) + +\Pi\big(\beta_{i,2}\big)}, \tag{61}$$

where

$$\Gamma_{i,3} = \varphi_{i,3}P_i|\mathbf{u}_{i,3}\mathbf{f}_i|^2 - \Upsilon_{i,3}|\mathbf{u}_{i,4}|^2, \tag{62}$$
$$\Pi\big(\beta_{i,1}\big) = \frac{BW\zeta_{i,1}}{\ln 2\beta_{i,1}}\gamma_{i,1} + \varphi_{i,1}\gamma_{i,1}^{\min}P_i|\mathbf{u}_{i,1}\mathbf{f}_i|^2 + \Upsilon_{i,1}|\mathbf{u}_{i,2}|^2, \tag{63}$$

and

$$\Pi\big(\beta_{i,2}\big) = \frac{BW\zeta_{i,2}}{\ln 2\beta_{i,2}}\gamma_{i,2} + \varphi_{i,2}\gamma_{i,2}^{\min}P_i|\mathbf{u}_{i,2}\mathbf{f}_i|^2 + \Upsilon_{i,2}|\mathbf{u}_{i,3}|^2. \tag{64}$$

Therefore, the closed-form expression for the *k*-th NOMA-BF user in a cluster can be derived as presented in Eq. (32).

REFERENCES

[1] R. Alghamdi *et al.*, "Intelligent surfaces for 6G wireless networks: A survey of optimization and performance analysis techniques," *IEEE Access*, vol. 8, pp. 202795–202818, 2020.

[2] Q. Wu and R. Zhang, "Towards smart and reconfigurable environment: Intelligent reflecting surface aided wireless network," *IEEE Commun. Mag.*, vol. 58, no. 1, pp. 106–112, Jan. 2020.

[3] C. Huang *et al.*, "Holographic MIMO surfaces for 6G wireless networks: Opportunities, challenges, and trends," *IEEE Wireless Commun.*, vol. 27, no. 5, pp. 118–125, Oct. 2020.

[4] Z. Li, W. Chen, and H. Cao, "Beamforming design and power allocation for transmissive RMS-based transmitter architectures," *IEEE Wireless Commun. Lett.*, vol. 11, no. 1, pp. 53–57, Jan. 2022.

[5] Q. Wu and R. Zhang, "Intelligent reflecting surface enhanced wireless network via joint active and passive beamforming,"*IEEE Trans. Wireless Commun.*, vol. 18, no. 11, pp. 5394–5409, Nov. 2019.

[6] D. Xu, X. Yu, Y. Sun, D. W. K. Ng, and R. Schober, "Resource allocation for IRS-assisted full-duplex cognitive radio systems,"*IEEE Trans. Commun.*, vol. 68, no. 12, pp. 7376–7394, Dec. 2020.

[7] X. Yu, D. Xu, Y. Sun, D. W. K. Ng, and R. Schober, "Robust and secure wireless communications via intelligent reflecting surfaces," *IEEE J. Sel. Areas Commun.*, vol. 38, no. 11, pp. 2637–2652, Nov. 2020.

[8] Y. Liu *et al.*, "Evolution of NOMA toward next generation multiple access (NGMA) for 6G," *IEEE J. Sel. Areas Commun.*, vol. 40, no. 4, pp. 1037–1071, Apr. 2022.

[9] A. Ihsan, W. Chen, S. Zhang, and S. Xu, "Energy-efficient NOMA multicasting system for beyond 5G cellular V2X communications with imperfect CSI," *IEEE Trans. Intell. Transp. Syst.*, vol. 23, no. 8, pp. 10721–10735, Aug. 2022.

[10] Z. Ding and H. V. Poor, "A simple design of IRS-NOMA transmission," *IEEE Commun. Lett.*, vol. 24, no. 5, pp. 1119–1123, May 2020.

[11] M. Fu, Y. Zhou, and Y. Shi, "Intelligent reflecting surface for downlink non-orthogonal multiple access networks,"in *Proc. IEEE Globecom Workshops*, Waikoloa, HI, USA, Dec. 2019, pp. 1–6.

[12] X. Mu, Y. Liu, L. Guo, J. Lin, and N. Al-Dhahir, "Exploiting intelligent reflecting surfaces in NOMA networks: Joint beamforming optimization," *IEEE Trans. Wireless Commun.*, vol. 19, no. 10, pp. 6884–6898, Oct. 2020.

[13] Y. Li, M. Jiang, Q. Zhang, and J. Qin, "Joint beamforming design in multi-cluster MISO NOMA reconfigurable intelligent surface-aided downlink communication networks," *IEEE Trans. Commun.*, vol. 69, no. 1, pp. 664–674, Jan. 2021.

[14] B. Zheng, Q. Wu, and R. Zhang, "Intelligent reflecting surface-assisted multiple access with user pairing: NOMA or OMA?" *IEEE Commun. Lett.*, vol. 24, no. 4, pp. 753–757, Apr. 2020.

[15] X. Mu, Y. Liu, L. Guo, J. Lin, and H. V. Poor, "Intelligent reflecting surface enhanced multi-UAV NOMA networks," *IEEE J. Sel. Areas Commun.*, vol. 39, no. 10, pp. 3051–3066, Oct. 2021.

[16] Z. Li, W. Chen, Q. Wu, K. Wang, and J. Li, "Joint beamforming design and power splitting optimization in IRS-assisted SWIPT NOMA networks," *IEEE Trans. Wireless Commun.*, vol. 21, no. 3, pp. 2019–2033, Mar. 2022.

[17] Q. Wu, X. Zhou, and R. Schober, "IRS-assisted wireless powered NOMA: Do we really need different phase shifts in DL and UL?" *IEEE Wireless Commun. Lett.*, vol. 10, no. 7, pp. 1493–1497, Jul. 2021.

[18] Q. Wang, F. Zhou, H. Hu, and R. Q. Hu, "Energy-efficient design for IRS-assisted MEC networks with NOMA," in *Proc. 13th Int. Conf. Wireless Commun. Signal Process. (WCSP)*, 2021, pp. 1–6.

[19] J. Zuo, Y. Liu, L. Yang, L. Song, and Y.-C. Liang, "Reconfigurable intelligent surface enhanced NOMA assisted backscatter communication system," *IEEE Trans. Veh. Technol.*, vol. 70, no. 7, pp. 7261–7266, Jul. 2021.

[20] C. Gong, X. Yue, X. Wang, X. Dai, R. Zou, and M. Essaaidi, "Intelligent reflecting surface aided secure communications for NOMA networks," *IEEE Trans. Veh. Technol.*, vol. 71, no. 3, pp. 2761–2773, Mar. 2022.

[21] M. Z. Chowdhury, M. Shahjalal, S. Ahmed, and Y. M. Jang, "6G wireless communication systems: Applications, requirements, technologies, challenges, and research directions," *IEEE Open J. Commun. Soc.*, vol. 1, pp. 957–975, 2020.

[22] B. Kimy *et al.*, "Non-orthogonal multiple access in a downlink multiuser beamforming system," in *Proc. IEEE Military Commun. Conf.*, 2013, pp. 1278–1283.

[23] Y. Liu, X. Mu, X. Liu, M. Di Renzo, Z. Ding, and R. Schober, "Reconfigurable intelligent surface (RIS) aided multi-user networks: Interplay between NOMA and RIS," 2020, *arXiv:2011.13336*.

[24] J. Zuo, Y. Liu, E. Basar, and O. A. Dobre, "Intelligent reflecting surface enhanced millimeter-wave NOMA systems," *IEEE Commun. Lett.*, vol. 24, no. 11, pp. 2632–2636, Nov. 2020.

[25] Z. Li, W. Chen, Q. Wu, H. Cao, K. Wang, and J. Li, "Robust beamforming design and time allocation for IRS-assisted wireless powered communication networks," *IEEE Trans. Commun.*, vol. 70, no. 4, pp. 2838–2852, Apr. 2022.

[26] G. Zhou, C. Pan, H. Ren, K. Wang, and A. Nallanathan, "A framework of robust transmission design for IRS-aided MISO communications with imperfect cascaded channels," *IEEE Trans. Signal Process.*, vol. 68, pp. 5092–5106, Aug. 2020, doi: 10.1109/TSP.2020.3019666.

[27] M. S. Ali, H. Tabassum, and E. Hossain, "Dynamic user clustering and power allocation for uplink and downlink non-orthogonal multiple access (NOMA) systems," *IEEE Access*, vol. 4, pp. 6325–6343, 2016.

[28] Q. Shi, L. Liu, W. Xu, and R. Zhang, "Joint transmit beamforming and receive power splitting for MISO SWIPT systems," *IEEE Trans. Wireless Commun.*, vol. 13, no. 6, pp. 3269–3280, Jun. 2014.

[29] J. Papandriopoulos and J. S. Evans, "SCALE: A low-complexity distributed protocol for spectrum balancing in multiuser DSL networks," *IEEE Trans. Inf. Theory*, vol. 55, no. 8, pp. 3711–3724, Aug. 2009.

[30] K. Shen and W. Yu, "Fractional programming for communication systems—Part I: Power control and beamforming," *IEEE Trans. Signal Process.*, vol. 66, no. 10, pp. 2616–2630, May 2018.

[31] M. R. Zamani, M. Eslami, M. Khorramizadeh, and Z. Ding, "Energy-efficient power allocation for NOMA with imperfect CSI," *IEEE Trans. Veh. Technol.*, vol. 68, no. 1, pp. 1009–1013, Jan. 2019.

Asim Ihsan received the B.S. degree in telecommunication engineering from the University of Engineering and Technology, Peshawar, Pakistan, in 2015, and the M.S. degree in information and communication engineering from Xi'an Jiaotong University, Xi'an, China, in 2018. He is currently pursuing the Ph.D. degree in information and communication engineering with Shanghai Jiao Tong University, Shanghai, China. His current research interests include the intelligent reflective surfaces, Internet of Vehicles, backscatter communications, physical layer security, and wireless sensor networks. He is an active reviewer of peer reviewed international journals.

Wen Chen (Senior Member, IEEE) is a Tenured Professor with the Department of Electronic Engineering, Shanghai Jiao Tong University, China, where he is the Director of Broadband Access Network Laboratory. He is a Fellow of Chinese Institute of Electronics and the Distinguished Lecturer of IEEE Communications Society and IEEE Vehicular Technology Society. He is the Shanghai Chapter Chair of IEEE Vehicular Technology Society, the Editor of IEEE TRANSACTIONS ON WIRELESS COMMUNICATIONS, IEEE TRANSACTIONS ON COMMUNICATIONS, IEEE ACCESS, and IEEE OPEN JOURNAL OF VEHICULAR TECHNOLOGY. His research interests include multiple access, wireless AI, and meta-surface communications. He has published more than 120 papers in IEEE journals and more than 120 papers in IEEE Conferences, with citations more than 8000 in Google scholar.

Muhammad Asif was born in Rahim Yar Khan, Bahawalpur Division, Pakistan, in 1990. He received the B.Sc. degree in telecommunication engineering from the Islamia University of Bahawalpur, Punjab, Pakistan, in 2013, and the master's degree in communication and information systems from Northwestern Polytechnical University, Xi'an, Shaanxi, China, in 2015, and the Ph.D. degree in information and communication engineering from the University of Science and Technology of China, Hefei, Anhui, China, in 2019. He is currently working as a Postdoctoral Researcher with the Department of Electronics and Information Engineering, Shenzhen University, Shenzhen, Guangdong, China. He has authored/coauthored several journal and conference papers. His research interests include wireless communication, channel coding, coded-cooperative communication, optimization and resource allocation, backscatter-enabled wireless communication, and IRS-assisted next-generation IOT networks.

Wali Ullah Khan (Member, IEEE) received the master's degree in electrical engineering from COMSATS University Islamabad, Pakistan, in 2017, and the Ph.D. degree in information and communication engineering from Shandong University, Qingdao, China, in 2020. He is currently working with the Interdisciplinary Centre for Security, Reliability and Trust (SnT), University of Luxembourg, Luxembourg. He has authored/coauthored more than 90 publications, including international journals, peer-reviewed conferences, and book chapters. His research interests include convex/nonconvex optimizations, nonorthogonal multiple access, reflecting intelligent surfaces, ambient backscatter communications, Internet of Things, intelligent transportation systems, satellite communications, unmanned aerial vehicles, physical layer security, and applications of machine learning.

Qingqing Wu (Senior Member, IEEE) received the B.Eng. and Ph.D. degrees in electronic engineering from the South China University of Technology and Shanghai Jiao Tong University (SJTU) in 2012 and 2016, respectively. He is currently an Assistant Professor with the State key laboratory of Internet of Things for Smart City, University of Macau.

From 2016 to 2020, he was a Research Fellow with the Department of Electrical and Computer Engineering, National University of Singapore. He has coauthored more than 100 IEEE journal papers with 26 ESI highly cited papers and 8 ESI hot papers, which have received more than 15000 Google citations. His current research interest includes intelligent reflecting surface, unmanned aerial vehicle (UAV) communications, and MIMO transceiver design. He was listed as the Clarivate ESI Highly Cited Researcher in 2021, the Most Influential Scholar Award in AI-2000 by Aminer in 2021 and the World's Top 2% Scientist by Stanford University in 2020 and 2021. He was a recipient of the IEEE Communications Society Young Author Best Paper Award in 2021, the Outstanding Ph.D. Thesis Award of China Institute of Communications in 2017, the Outstanding Ph.D. Thesis Funding in SJTU in 2016, the IEEE ICCC Best Paper Award in 2021, and IEEE WCSP Best Paper Award in 2015. He was the Exemplary Editor of IEEE COMMUNICATIONS LETTERS in 2019 and the exemplary reviewer of several IEEE journals. He serves as an Associate Editor for IEEE TRANSACTIONS ON COMMUNICATIONS, IEEE COMMUNICATIONS LETTERS, IEEE WIRELESS COMMUNICATIONS LETTERS, IEEE OPEN JOURNAL OF COMMUNICATIONS SOCIETY (OJ-COMS), and IEEE OPEN JOURNAL OF VEHICULAR TECHNOLOGY (OJVT). He is the Lead Guest Editor for IEEE JOURNAL ON SELECTED AREAS IN COMMUNICATIONS on "UAV Communications in 5G and Beyond Networks," and the Guest Editor for IEEE OPEN JOURNAL OF VEHICULAR TECHNOLOGY on "6G Intelligent Communications" and IEEE OPEN JOURNAL OF COMMUNICATIONS SOCIETY on "Reconfigurable Intelligent Surface-Based Communications for 6G Wireless Networks." He is the Workshop Co-Chair for IEEE ICC 2019–2022 workshop on "Integrating UAVs into 5G and Beyond" and the IEEE GLOBECOM 2020 and ICC 2021 workshop on "Reconfigurable Intelligent Surfaces for Wireless Communication for Beyond 5G." He serves as the Workshops and Symposia Officer of Reconfigurable Intelligent Surfaces Emerging Technology Initiative and Research Blog Officer of Aerial Communications Emerging Technology Initiative. He is the IEEE Communications Society Young Professional Chair in Asia Pacific Region.

Jun Li (Senior Member, IEEE) received the Ph.D. degree in electronic engineering from Shanghai Jiao Tong University, Shanghai, China, in 2009. From January 2009 to June 2009, he worked with the Department of Research and Innovation, Alcatel Lucent Shanghai Bell, as a Research Scientist. From June 2009 to April 2012, he was a Post-Doctoral Fellow with the School of Electrical Engineering and Telecommunications, University of New South Wales, Australia. From April 2012 to June 2015, he was a Research Fellow with the School of Electrical Engineering, The University of Sydney, Australia. Since June 2015, he has been a Professor with the School of Electronic and Optical Engineering, Nanjing University of Science and Technology, Nanjing, China. He was a Visiting Professor with Princeton University from 2018 to 2019. His research interests include network information theory, game theory, distributed intelligence, multiple agent reinforcement learning, and their applications in ultra-dense wireless networks, mobile edge computing, network privacy and security, and the Industrial Internet of Things. He has coauthored more than 200 papers in IEEE journals and conferences and holds one U.S. patents and more than ten Chinese patents in these areas. He received an Exemplary Reviewer of IEEE TRANSACTIONS ON COMMUNICATIONS in 2018 and the Best Paper Award from IEEE International Conference on 5G for Future Wireless Networks in 2017. He is an Editor of IEEE TRANSACTIONS ON WIRELESS COMMUNICATIONS and IEEE COMMUNICATION LETTERS and a TPC Member for several flagship IEEE conferences.